

Quasimolecular states in ^{24}Mg and d - α angular correlations in the $^{12}\text{C}(^{14}\text{N},d)^{24}\text{Mg}^*(\alpha)^{20}\text{Ne}$ reaction

T. L. Belyaeva^{1,2,*} and N. S. Zelenskaya¹¹*D. V. Skobeltsyn Institute of Nuclear Physics, M. V. Lomonosov Moscow State University, RU-119899 Moscow, Russian Federation*²*Universidad Autonoma del Estado de México, 50000 Toluca, México*

(Received 9 May 2002; published 6 September 2002)

Theoretical approach for studies on particle-particle angular correlations in nuclear reactions induced by light and semiheavy ions with an incident energy up to 10 MeV/nucleon is developed. The generalized methods for calculations of the angular correlation functions and the spin tensors of the density matrix for the reaction products based on the distorted-wave model with finite interaction range and the compound nucleus model are presented for reactions involving high-lying excited states. The differential cross sections and d - α correlation functions in the $^{12}\text{C}(^{14}\text{N},d)^{24}\text{Mg}^*(\alpha)^{20}\text{Ne}$ reaction induced by ^{14}N ions at $E_{lab}=29$ – 45 MeV are analyzed both in the framework of the model of direct ^{12}C transfer and the statistical compound nucleus model. The reduced width amplitudes for the higher-excited states in ^{24}Mg with $^{12}\text{C}\otimes^{12}\text{C}$ quasimolecular structure are extracted. The importance of relative motion of $^{12}\text{C}+^{12}\text{C}^*$ nuclei is demonstrated.

DOI: 10.1103/PhysRevC.66.034604

PACS number(s): 25.70.Hi, 25.70.Gh, 27.30.+t, 21.10.Jx

I. INTRODUCTION

Experimental and theoretical studies of nuclear molecular states in the heavy ion reactions have been conducted since the beginning 1960s, when nuclear quasimolecules were experimentally discovered by Bromley, Kuehner, and Almqvist [1,2] in the $^{12}\text{C}+^{12}\text{C}$ system. It was found that these unexpectedly narrow and well-separated resonances in the interaction of heavy ions are well correlated in different channels and that their widths are much greater than for the compound-nucleus (CN) ones for a given excitation energy (around 15–50 MeV) of the CN system [1,2]. During last decades the search for resonance phenomena has been extended to the more heavier symmetric and asymmetric systems (which feature even N and even Z nuclei) primarily in elastic and inelastic scattering and in reactions leading to α -particle transfer channels [3–6]. The light and semiheavy-ion grazing collisions can form states with very high angular momentum, and these states are associated with quasimolecular configurations of two rotating nuclei. In the recent studies [7–9], the breakup reactions induced by light ions are associated with fissionlike decay of the quasimolecular state into two heavy fragments, for example, $^{24}\text{Mg}\rightarrow^{12}\text{C}+^{12}\text{C}$ or $^{24}\text{Mg}\rightarrow^{16}\text{O}+^8\text{Be}$. It was suggested that an enhanced sensitivity to the state with a strongly deformed quasimolecular configuration can be achieved in experiments.

Original microscopic model has been developed to describe moleculelike $^{12}\text{C}+^{12}\text{C}$ structure in ^{24}Mg [10,11]. The recent experimental results in this field and theoretical models describing nuclear quasimolecules are summarized in the book of Greiner, Park, and Scheid [12] and review of Betts and Wuosmaa [13].

Experimental and theoretical investigations of the particle-particle angular correlations and the final state polar-

ization of nuclei in multinucleon transfer reactions induced by light and semiheavy ions with nontrivial spins [14–22], opened up a new chapter in the study of the cluster and quasimolecular nuclear states and the reaction mechanisms. Thus, it should be emphasized that in the collision of nuclei possessing spins the interaction is, in general, noncentral and it depends on the relative orientation of spins. In particular, when mechanism for final-nucleus formation is different from statistical evaporation, the final nucleus with nonzero spin is oriented and the population of the magnetic substates becomes nonuniform. When the final nucleus is formed in an excited state, its decay becomes anisotropic too. Nevertheless, in binary reactions it is possible to restore completely all the components of the density matrix of a final nuclear state by measuring the angular correlation functions in several reaction planes [14].

Historically, the study of particle-particle angular correlations began with investigations of the quasielastic knockout reactions $A(p,2p)B^*$ on light nuclei [23] and the clustering phenomena in light nuclei by the (a,ax) reactions [24,25]. Important quantitative spectroscopic information and new theoretical results were obtained recently in Refs. [26,27], where the quasielastic knockout of α clusters by intermediate energy protons and ultrarelativistic electrons was studied in details.

As early as in 1984, Artemov *et al.* [15] obtained experimental data for the d - α angular correlation functions (ACFs) in the $^{12}\text{C}(^{14}\text{N},d)^{24}\text{Mg}^*(\alpha)^{20}\text{Ne}$ reaction. These data have attracted considerable interest to the study of quasimolecular states of nuclei via particle-particle angular correlations. It was found that for the excited state 13.45 MeV ($J^\pi=6^+$) in ^{24}Mg there exist oscillations in ACF at forward deuteron emission angles, whose shape is well described by the square of the sixth-order Legendre polynomial and could not be explained by the CN model. The authors interpreted this fact as the proof of direct transfer of 12 nucleons and suggested the presence of quasimolecular $^{12}\text{C}\otimes^{12}\text{C}$ configurations in this state of ^{24}Mg . This result was confirmed ones again in

*Corresponding author. FAX: +52 72 22 96 55 54. Email address: beltanya01@yahoo.com

1994 by Zurmuhle *et al.* [19]. Moreover, the exact finite-range DWBA (EFR-DWBA) calculations of the differential cross sections assuming the direct-carbon-transfer mechanism [28,29] demonstrated that, in general, this model gives a good agreement with the experimental data. Whereas the analysis of the deuteron angular distributions as well as d - α ACFs assuming the Hauser-Feshbach formalism for the CN model [30] confirmed the importance of CN contribution and demonstrated the smooth monotonic behavior of the calculated d - α ACFs for the 13.45-MeV(6^+) state in ^{24}Mg for forward deuteron emission angles.

Nevertheless, a number of important questions still remained. Why was a polynomial structure of the ACFs observed only for one selected state in ^{24}Mg and was not observed for other states with high spin near this state? Is it only exception rather than the rule? What is the origin of the energy dependence of the ACFs for this state? What is the reaction mechanism that makes the main contribution to the reaction cross sections and ACFs? These questions are taken up in this paper.

Our study focuses on the theoretical analysis of different reaction characteristics and their relation with the quasimolecular states in ^{24}Mg for excitation energies of $E^* = 8-14$ MeV. We calculate the differential cross sections as well as d - α ACFs in $^{12}\text{C}(^{14}\text{N},d)^{24}\text{Mg}^*(a)^{20}\text{Ne}$ to obtain the full description of experimental data reported to date and to answer the questions mentioned above.

In Sec. II of the paper, the basic mathematical formalism of ACF calculation for massive transfer mechanisms in EFR-DWBA and for the CN model in the Hauser-Feshbach formalism is developed. Section III of the paper focuses on investigations of the $^{12}\text{C}(^{14}\text{N},d)^{24}\text{Mg}^*(\alpha)^{20}\text{Ne}$ reaction cross sections and ACFs and on the numerical calculations of quasimolecular $^{12}\text{C} \otimes ^{12}\text{C}^*$ states in ^{24}Mg . The quantitative values of the reduced width amplitudes (RWAs) for the $^{12}\text{C} \otimes ^{12}\text{C}$ configurations are extracted, and contributions of the different reaction mechanisms are compared.

II. GENERAL METHODS FOR CALCULATIONS OF THE PARTICLE-PARTICLE ANGULAR CORRELATION FUNCTIONS BASED ON THE SPIN DENSITY MATRIX AND ITS SPIN TENSORS

A. General formalism

Let us study the differential cross sections and angular correlation functions in reactions induced by light and semi-heavy ions in the framework of the general theory of angular correlations in terms of the spin density matrix $\rho_I(M, M')$ developed in the classic works of Biedenharn and Rose [31], and Goldfarb [32]. The spin density matrix characterizes the orientational properties of a system in the spin space and can be obtained by integration of the complete wave function $\Psi_I(\mathbf{r}, M)$ of a system with spin I and a spin projection M over the radial variable

$$\rho_I(M, M') = \int d\mathbf{r} |\Psi_I(\mathbf{r}, M')\rangle \langle \Psi_I(\mathbf{r}, M)|. \quad (1)$$

In a nonoriented system, all the spin states are populated with equal probability

$$\rho_I(M, M') = \frac{\delta_{MM'}}{2I+1}, \quad (2)$$

where the following normalization condition for the density matrix is used:

$$\text{Tr } \rho_I(M, M') = 1. \quad (3)$$

For a binary nuclear reaction $A(a,b)B$ the relation between the spin density matrices of the system before and after the collision ρ_i and ρ_f is determined (like that between the initial and final wave functions of the system) in terms of the transition amplitude T_{if} :

$$\rho_f = \langle T_{if} \rho_i T_{if}^\dagger \rangle. \quad (4)$$

In the initial state the nuclei are independent, and therefore ρ_i factorizes into two parts corresponding to the projectile and target. In the case of unpolarized incident particles and targets the initial system is nonoriented and thus, according to Eq. (2), all the spin projections are populated with equal probability and the spin density matrices of the initial nuclei are diagonal. To obtain the density matrix of the final system we extract the spin density matrix ρ_{I_f} of the final nucleus B^* and average over the spin projections of the emergent particle. Then the spin density matrix of the nucleus B^* in the state with spin I_f and projection M_f may be written as

$$\begin{aligned} \rho_{I_f}(M_f, M'_f) &= \frac{1}{(2I_a+1)(2I_A+1)} \\ &\times \sum_{M_a M_A M_b M'_b} T_{if, M_a M_A M_b M_f} T_{if, M_a M_A M'_b M'_f}^* \end{aligned} \quad (5)$$

For practical applications it is convenient to introduce the spin tensors $\rho_{kq}(I_f)$ of the density matrix, which are defined by the standard manner

$$\begin{aligned} \rho_{kq}(I_f) &= \sqrt{2I_f+1} \sum_{M_f M'_f} (-1)^{I_f-M'_f} \\ &\times \langle I_f M'_f I_f - M_f | k q \rangle \rho_{I_f}(M_f, M'_f), \end{aligned} \quad (6)$$

where $0 < k < 2I_f$ and $q = -k, \dots, k$.

If the spin density matrices of initial nonoriented nuclei satisfy the normalization condition (3), the spin density matrix (5) is normalized to the differential cross section

$$\text{Tr } \rho_{I_f}(M_f, M'_f) = \frac{d\sigma}{d\Omega} = \rho_{00}. \quad (7)$$

This important property of the monopole spin tensor directly follows from Eq. (6).

Spin tensors of the spin density matrix for excited nuclear states and other characteristics of an oriented system can be obtained by studying the angular correlation functions of reaction products.

Let us consider a two stage nuclear process, the first stage of which, $a(I_a) + A(I_A) \rightarrow B^*(I_f) + b(I_b)$, is the binary nuclear reaction, where the nucleus B^* is produced in an excited state. The second stage of the process is the decay $B^*(I_f) \rightarrow C(I_0) + c(I_c)$, where C is the residual nucleus and c is the secondary emission of particle or γ quantum (the total nuclear spins are shown in brackets). According to the general formalism, the angular correlation function, $W(\Omega_b, \Omega_c)$ is defined as the probability for simultaneous detection of particle b emitted in the direction \vec{n}_1 and particle c emitted in the direction \vec{n}_2 . The function $W(\Omega_b, \Omega_c)$ is defined in terms of the spin density matrix $\rho_{I_f}(M_f, M'_f)$ of the final nucleus $B^*(I_f)$ and the matrix $\varepsilon_{I_f}(M_f, M'_f)$ of the emitted particle detection efficiency:

$$W(\vec{n}_1, \vec{n}_2) \equiv W(\Omega_b, \Omega_c) = \text{Tr}(\varepsilon_{I_f}^* \rho_{I_f}). \quad (8)$$

One can obtain an alternative form for the function (8) using the spin tensors $\rho_{kq}(I_f)$ of the spin density matrix and the tensors $\varepsilon_{kq}(I_f; \Omega_c)$ of the efficiency matrix

$$W(\Omega_b, \Omega_c) = \sum_{kq} \rho_{kq}(I_f, \Omega_b) \varepsilon_{kq}^*(I_f, \Omega_c). \quad (9)$$

The system $B^*(I_f) \rightarrow C^*(I_0) + c(I_c)$ is described by the angular-momentum coupling scheme

$$\mathbf{I}_f = \mathbf{I}_0 + \mathbf{I}_c + \mathbf{L} = \mathbf{S} + \mathbf{L}, \quad (10)$$

where L is the orbital angular momentum of the relative motion of decay products, and S is the channel spin.

When spin states of the residual nucleus C and the emitted particle c are not fixed or all their spin states are populated with equal probability, the tensors of the efficiency matrix take the form [18,21]

$$\varepsilon_{kq}(I_f; \Omega_c) = (2I_f + 1) \sum_{SLL'} (-1)^{I_f+S} \sqrt{\frac{(2L+1)(2L'+1)}{(2k+1)(2I_c+1)}} \\ \times \langle L0L'0 | k0 \rangle w(LI_f L' I_f; Sk) Y_{kq}^*(\Omega_c). \quad (11)$$

In a special case of the zero spin I_c of the emitted particle (for example, in a case of α -particle decay of the excited nuclear state) and the zero spin I_0 of the residual nucleus C , the tensors $\varepsilon_{kq}(I_f)$ take the more simple form

$$\varepsilon_{kq}(I_f; \Omega_c) = (-1)^{I_f} (2I_f + 1) [4\pi(2k+1)]^{-1/2} \\ \times \langle I_f 0 I_f 0 | k0 \rangle Y_{kq}^*(\Omega_c). \quad (12)$$

In this case the equation for the angular correlation function results from Eqs. (5), (6), and (12),

$$W(\Omega_b, \Omega_c) = \frac{(2I_f + 1)^{1/2}}{(2I_a + 1)(2I_A + 1)} \\ \times \sum_{M_f M'_f} (-1)^{I_f} Y_{I_f M_f}^*(\Omega_c) Y_{I_f M'_f}(\Omega_c) \\ \times \sum_{M_a M_A M_b} |T_{if, M_a M_A M_b M_f}(\Omega_b)|^2. \quad (13)$$

If one of the decay products has nonzero spin, then more general expressions for the tensors of efficiency matrix and general Eqs. (8), (9) for the ACFs may be used (see, for example, the $^6\text{Li}^*$ polarization tensors measurements and calculations via α - α_1 angular correlations presented in the paper [21]).

Two general methods for calculations of the spin tensors of density matrix and the ACFs are considered in our work, they are the exact finite-range DWBA (EFR-DWBA) and the modified Hauser-Feshbach (HF) methods of statistical CN model.

B. Mathematical formalism for calculations of the angular correlation functions in the exact finite range DWBA

In the EFR-DWBA the transition amplitude T_{if} of the reaction $A(a, b)B$ is given by [33]

$$T_{if}(\Omega_b) = \frac{1}{\sqrt{E_i E_f}} \frac{K_b}{K_a} \int \int d\mathbf{r}_a d\mathbf{r}_b \chi^{(-)}(\mathbf{K}_b \mathbf{r}_b) \mathcal{I} \chi^{(+)}(\mathbf{K}_a \mathbf{r}_a), \quad (14)$$

where $\chi^{(+)}(\mathbf{K}_a \mathbf{r}_a)$ and $\chi^{(-)}(\mathbf{K}_b \mathbf{r}_b)$ are distorted waves in the entrance and exit reaction channels, $\mathcal{I} = \langle \Psi_B \Psi_b | \mathbf{V} | \Psi_A \Psi_a \rangle$ is the overlap integral of the internal wave functions $\Psi_B, \Psi_b, \Psi_A, \Psi_a$ of the corresponding nuclei and the interaction potential \mathbf{V} . For the one-step *direct terms* (“breakup” of the projectile) \mathbf{V} contains the interaction potential for the direct stripping and heavy knock-on mechanisms. Finally, the transition amplitude T_{if} may be written as [34]

$$T_{if}(\Omega_b) = \frac{1}{\sqrt{E_i E_f}} \frac{K_b}{K_a} \\ \times \sum_{I_1 M_1 I_2 M_2 l m_l} (-1)^{I_1+M_2} [(2I_1+1)(2I_2+1)]^{1/2} \\ \times \langle I_A M_A I_1 M_1 | I_f M_f \rangle \langle I_b M_b I_2 M_2 | I_a M_a \rangle \\ \times \langle I_2 - M_2 I_1 M_1 | l m_l \rangle \sum_{\Lambda_1 \Lambda_2 I_X E_X} (-1)^{\Lambda_1 + \Lambda_2} \\ \times \Theta_{I \Lambda_1 \Lambda_2 I_1 I_2 I_X I_f} \beta_{l m_l \Lambda_1 \Lambda_2 I_X E_X}(\Omega_b). \quad (15)$$

The essence of the reaction mechanism is contained in the kinematical amplitudes $\beta_{l m_l \Lambda_1 \Lambda_2 I_X E_X}(\Omega_b)$, which are the overlap integrals of incoming and outgoing distorted waves, the wave functions of the relative motion, and the interaction potentials.

We write the structure factors $\Theta_{I\Lambda_1\Lambda_2I_1I_2I_XI_f}$ in terms of the RWAs; $\Theta_{\Lambda_1I_1I_XI_f}^{B\rightarrow X+A}$ and $\Theta_{\Lambda_2I_2I_XI_a}^{a\rightarrow X+b}$, which describe the probability of formation of the cluster configurations $X+A$ and $X+b$ containing the intermediate nucleus X in the nuclei B and a , respectively,

$$\begin{aligned} & \Theta_{I\Lambda_1\Lambda_2I_1I_2I_XI_f} \\ &= (-1)^{I_X} \frac{u(I_1\Lambda_1I_2\Lambda_2:I_XI)}{\sqrt{2I_X+1}} \Theta_{\Lambda_1I_1I_XI_f}^{B\rightarrow X+A} \Theta_{\Lambda_2I_2I_XI_a}^{a\rightarrow X+b}. \end{aligned} \quad (16)$$

The standard angular-momentum coupling scheme is used in Eqs. (15), (16)

$$\begin{aligned} \mathbf{I} &= \mathbf{\Lambda}_1 + \mathbf{\Lambda}_2 = \mathbf{I}_1 + \mathbf{I}_2, \\ \mathbf{I}_f &= \mathbf{I}_1 + \mathbf{I}_A, \quad \mathbf{I}_a = \mathbf{I}_2 + \mathbf{I}_b, \end{aligned} \quad (17)$$

where l is the transferred angular momentum, Λ_1 and Λ_2 are orbital angular momenta of relative motion of the clusters $A+X$ and $b+X$ in the nuclei B and a , respectively, and I_1 and I_2 are total transferred angular momenta.

Substituting Eq. (15) into Eq. (13), we write the expression for the ACF in the EFR-DWBA as

$$\begin{aligned} W(I_f; \Omega_b, \Omega_c) &= \frac{(2I_f+1)^{1/2}}{(2I_A+1)} \times \sum_{I_2M_2M_A} \left| \sum_{M_f} M_{I_2M_2M_A}^{I_fM_f}(\Omega_b) \right. \\ & \quad \left. \times Y_{I_fM_f}^*(\Omega_c) \right|^2, \end{aligned} \quad (18)$$

where

$$\begin{aligned} \theta_{\Lambda_2I_2I_XI_a}^{a\rightarrow X+b} &= \left(\frac{N_a}{N_X} \right)^{1/2} \left(\frac{a}{X} \right)^{N_{\Lambda_2}/2} \sum_{[f_i]L_iS_iT_i, i=a,b,X} a_{[f_a]L_aS_a}^{I_aT_a} \times a_{[f_X]L_XS_X}^{I_XT_X} a_{[f_b]L_bS_b}^{I_bT_b} K(\Lambda_2L_b; L_2) \\ & \quad \times \langle L_bM_{L_b}S_bM_{S_b} | I_bM_{I_b} \rangle \langle L_aM_{L_a}S_aM_{S_a} | I_aM_{I_a} \rangle \times \langle L_XM_{L_X}S_XM_{S_X} | I_XM_{I_X} \rangle \langle \Lambda_2\mu_2L_bM_{L_b} | L_2M_{L_2} \rangle \\ & \quad \times \langle L_XM_{L_X}L_2M_{L_2} | L_aM_{L_a} \rangle \\ & \quad \times \langle S_XM_{S_X}S_bM_{S_b} | S_aM_{S_a} \rangle \times \langle N_a[f_a]L_aS_aT_a | N_X[f_X]L_XS_XT_X; N_{\Lambda_2}\Lambda_2[f_b]L_bS_bT_b\{L_2\} \rangle \\ &= \sum_{J_2M_{J_2}} \Xi_{\Lambda_2I_XJ_2I_a}^{a\rightarrow X+b} \langle I_XM_{I_X}J_2M_{J_2} | I_aM_{I_a} \rangle \langle \Lambda_2\mu_2I_bM_{I_b} | J_2M_{J_2} \rangle, \end{aligned} \quad (21)$$

$$\begin{aligned} M_{I_2M_2M_A}^{I_fM_f}(\Omega_b) &= \sum_{I_1M_1} (2I_1+1)^{1/2} \langle I_A M_A I_1 M_1 | I_f M_f \rangle \\ & \quad \times \sum_{lm_1} i^l \langle I_2 - M_2 I_1 M_1 | lm_1 \rangle \\ & \quad \times \sum_{\Lambda_1\Lambda_2I_XE_X} (-1)^{I+\Lambda_1+\Lambda_2} \Theta_{I\Lambda_1\Lambda_2I_1I_2I_XI_f} \\ & \quad \times \beta_{lm_1\Lambda_1\Lambda_2I_XE_X}(\Omega_b). \end{aligned} \quad (19)$$

The expression (18) has been obtained here for the case when both the emitted particle c and residual nucleus C have zero spins. A similar analysis can be carried out for the non-zero spin case as well.

C. Structure factors

To calculate the structure factors let us start from the conventional definition of the cluster spectroscopic amplitude of reduced width for decay probability of the nuclei a and B via the channels $X+b$ and $X+A$, respectively (see, for example, Refs. [35,36]),

$$\begin{aligned} \theta_{\Lambda_2I_2I_XI_a}^{a\rightarrow X+b} &= \int \langle I_a T_a M_a | I_X T_X M_X | I_b T_b M_b \rangle \\ & \quad \times \Psi_{n_2\Lambda_2\mu_2}(\mathbf{r}_{Xb}) d\tau, \end{aligned} \quad (20)$$

where $\Psi_y = |I_y T_y M_y\rangle$, $y=a,b,X$, are the internal wave functions of the corresponding nuclei and $\Psi_{n_2\Lambda_2\mu_2}(\mathbf{r}_{Xb})$ is the wave function of relative motion of the nuclei $X+b$ in the initial nucleus a . In this section we shall refer to subscript 2 for a $a\rightarrow X+b$ vertex and subscript 1 for a $B\rightarrow X+A$ vertex, and we shall write expressions for RWAs for a $a\rightarrow X+b$ vertex, taking in the mind that for a $B\rightarrow X+A$ vertex the expressions are the same with the substitution $2\leftrightarrow 1$, $a\leftrightarrow B$, $b\leftrightarrow A$.

The general expression for the RWA in terms of the fractional parentage coefficients (FPC) in the translational invariant shell model technique is based on the transformation of the oscillatory wave functions [35–40]. For our present purposes, we rewrite the general expression to describe a possibility of formation of a massive cluster X possessing its own excited states

where

$$\begin{aligned} \Xi_{\Lambda_2 I_X J_2 I_a}^{a \rightarrow X+b} &= \left(\frac{N_a}{N_X} \right)^{1/2} \left(\frac{a}{X} \right)^{N_{\Lambda_2/2}} \times \sum_{[f_i] L_i S_i T_i, i=a,b,X} a_{[f_a] L_a S_a}^{I_a T_a} \\ &\times a_{[f_X] L_X S_X}^{I_X T_X} a_{[f_b] L_b S_b}^{I_b T_b} (-1)^{\Lambda_2 + I_X + I_b - I_a} \\ &\times u(\Lambda_2 L_b J_2 S_b; L_2 I_b) K(\Lambda_2 L_b; L_2) \\ &\times \langle T_X M_{T_X} T_b M_{T_b} | T_a M_{T_a} \rangle \begin{pmatrix} L_X & S_X & I_X \\ L_2 & S_b & J_2 \\ L_a & S_a & I_a \end{pmatrix} \\ &\times \langle N_a [f_a] L_a S_a T_a | N_X [f_X] L_X S_X T_X; N_2 [f_b] L_2 S_b T_b \rangle. \end{aligned} \quad (22)$$

In Eqs. (21), (22) $a_{[f_i] L_i S_i}^{J_i T_i}$ are the intermediate coupling coefficients and $K(\Lambda_2 L_b; L_2)$ are the generalized Talmi-Moshinsky-Smirnov coefficients [35–40], which extract the wave function $\Psi_{n_2 \Lambda_2 \mu_2}(\mathbf{r}_{Xb})$ of relative motion of the nuclei with the orbital angular momentum Λ_2 and the internal wave function with major quantum number n_b and the orbital angular momentum L_b from the wave function of b nucleons with the angular momentum L_2 (so $n_2 + n_b = N_2$).

Here we define the total angular momentum in a $a \rightarrow X + b$ vertex as

$$\mathbf{J}_2 = \mathbf{I}_a + \mathbf{I}_X = \Lambda_2 + \mathbf{I}_b = \mathbf{L}_2 + \mathbf{S}_b, \quad (23)$$

and we use the following coupling scheme for orbital angular momenta:

$$\mathbf{L}_a = \mathbf{L}_X + \Lambda_2 + \mathbf{I}_b = \mathbf{L}_X + \mathbf{L}_2. \quad (24)$$

Thus, it is convenient to express integral $\mathcal{I} = \langle \Psi_B \Psi_b | V | \Psi_A \Psi_a \rangle$ involving in the matrix element (14) in terms of the RWAs in the vertices $B \rightarrow X + A$ and $a \rightarrow X + b$:

$$\begin{aligned} \mathcal{I} &= \sum_{I_1 M_1 I_2 M_2} \langle I_A M_{I_A} I_1 M_{I_1} | I_f M_{I_f} \rangle \langle I_b M_{I_b} I_2 M_{I_2} | I_a M_{I_a} \rangle \\ &\times \sum_{\Lambda_1 \Lambda_2 I_X E_X} \langle \Lambda_2 \mu_2 I_X M_{I_X} | I_2 M_{I_2} \rangle \langle \Lambda_1 \mu_1 I_X M_{I_X} | I_1 M_{I_1} \rangle \\ &\times \Psi_{n_1 \Lambda_1 \mu_1}^*(\mathbf{r}_{XA}) V \Psi_{n_2 \Lambda_2 \mu_2}(\mathbf{r}_{Xb}) \Theta_{\Lambda_1 I_1 I_X}^{B \rightarrow X+A} \Theta_{\Lambda_2 I_2 I_X}^{a \rightarrow X+b} \end{aligned} \quad (25)$$

by defining

$$\Theta_{\Lambda_2 I_2 I_X I_a}^{a \rightarrow X+b} = \sum_{J_2} u(I_b \Lambda_2 I_a I_X; J_2 I_2) \Xi_{\Lambda_2 I_X J_2 I_a}^{a \rightarrow X+b}, \quad (26)$$

$$\Theta_{\Lambda_1 I_1 I_X I_f}^{B \rightarrow X+A} = \sum_{J_1} u(I_A \Lambda_1 I_f I_X; J_1 I_1) \Xi_{\Lambda_1 I_X J_1 I_f}^{B \rightarrow X+A} \quad (27)$$

and taking into account the total angular-momentum coupling schemes

$$\mathbf{I}_a = \mathbf{I}_X + \Lambda_2 + \mathbf{I}_b = \mathbf{I}_X + \mathbf{J}_2 = \mathbf{I}_2 + \mathbf{I}_b, \quad (28)$$

$$\mathbf{I}_f = \mathbf{I}_X + \Lambda_1 + \mathbf{I}_A = \mathbf{I}_X + \mathbf{J}_1 = \mathbf{I}_1 + \mathbf{I}_A. \quad (29)$$

Now we rewrite the integral (25) by introducing a sum on the transferred orbital angular momentum l in the standard form

$$\begin{aligned} \mathcal{I} &= \sum_{l m_l I_1 M_1 I_2 M_2} \sqrt{(2I_1+1)(2I_2+1)} \langle I_A M_{I_A} I_1 M_{I_1} | I_f M_{I_f} \rangle \\ &\times \langle I_b M_{I_b} I_2 M_{I_2} | I_a M_{I_a} \rangle \langle I_2 - M_{I_2} I_1 M_{I_1} | l m_l \rangle \\ &\times \sum_{\Lambda_1 \Lambda_2 I_X E_X} \Theta_{l \Lambda_1 \Lambda_2 I_1 I_2 I_X I_f} \times \mathbf{f}_{l m_l \Lambda_1 \Lambda_2 I_X E_X}, \end{aligned} \quad (30)$$

where the structure factors $\Theta_{l \Lambda_1 \Lambda_2 I_1 I_2 I_X I_f}$ correspond to Eq. (16) and form factors $\mathbf{f}_{l m_l \Lambda_1 \Lambda_2 I_X E_X}$ are given by

$$\begin{aligned} \mathbf{f}_{l m_l \Lambda_1 \Lambda_2 I_X E_X} &= \sum_{\mu_1 \mu_2} (-)^{\mu_1} \langle \Lambda_1 \mu_1 \Lambda_2 - \mu_2 | l m_l \rangle \\ &\times \Psi_{n_1 \Lambda_1 \mu_1}^*(\mathbf{r}_{XA}) \mathbf{V} \Psi_{n_2 \Lambda_2 \mu_2}(\mathbf{r}_{Xb}). \end{aligned} \quad (31)$$

Thus, without changing the formal structure of the EFR-DWBA formalism, we are able to consider here the case of a transferred massive cluster X , which possesses its own excited states.

D. Spin tensors of the density matrix and the angular correlation functions in the statistical CN model

The statistical CN theory based on the Hauser-Feshbach formalism [41] successfully describes the cross sections for such reactions, which are characterized by the smooth, non-resonance energy and angular dependences. In this case the incident particle energy is distributed according to the statistical mechanics laws for over all the nuclear degrees of freedom, i.e., thermodynamical equilibrium is established in the system. When the reaction is induced by a particle of sufficiently high energy, the excited levels of CN in the continuum will give the most important contribution to the reaction cross section. Consequently, the calculation of the cross section for the reaction $A(a,b)B$ in the HF formalism is reduced to the calculation of the transmission coefficients $\mathcal{T}_{II}^{I,C}$ for the various channels, defined as the ratio of the number of particles passing through the nuclear barrier into the interior of the nucleus to the number of incident particles.

Let us consider the method for calculation of the spin tensors of the density matrix and ACFs in the modified statistical CN model [42], which allows us to investigate the interaction between nuclei with arbitrary spins including the spin-orbit interaction. We begin with the usual expression for the transition amplitude T_{if} of the reaction $A(a,b)B$

$$T_{if} = \langle \Psi_f | \Psi_C \rangle \langle \Psi_C | \Psi_i \rangle. \quad (32)$$

The wave functions Ψ_i, Ψ_f , and Ψ_C of initial, final, and compound quasistationary state λ with spin I_C , level energy E_λ , and total width Γ_λ can be written by using the reduced width technique as follows:

$$\Psi_i = \Psi_A \Psi_a \chi^{(+)}(\mathbf{K}_a \mathbf{r}_a), \quad (33)$$

$$\Psi_f = \Psi_B \Psi_b \chi^{(-)}(\mathbf{K}_b \mathbf{r}_b),$$

$$\Psi_C(\mathbf{r}, E_\lambda) = \frac{1}{(E_\lambda - E) + \frac{i}{2} \Gamma_\lambda} \Psi_C(\mathbf{r}),$$

$$\begin{aligned} \Psi_C(\mathbf{r}) &= \sum_{I_1 M_{I_1} I_C M_C} \langle I_a M_{I_a} I_A M_{I_A} | I_1 M_{I_1} \rangle \\ &\times \langle I_1 M_{I_1} l_a m_a | I_C M_{I_C} \rangle \theta_{l_a l_a I_1}^{C(\lambda) \rightarrow A+a} \Psi_A \Psi_a \Psi_{l_a}(\mathbf{r}_a) \\ &= \sum_{I_2 M_{I_2} I_C M_C} \langle I_b M_{I_b} I_f M_{I_f} | I_2 M_{I_2} \rangle \\ &\times \langle I_2 M_{I_2} l_b m_b | I_C M_{I_C} \rangle \theta_{l_b l_b I_2}^{C(\lambda) \rightarrow B+b} \Psi_B \Psi_b \Psi_{l_b}(\mathbf{r}_b), \end{aligned}$$

where $\chi^{(+)}(\mathbf{K}_a \mathbf{r}_a)$ and $\chi^{(-)}(\mathbf{K}_b \mathbf{r}_b)$ are the distorted waves in the entrance and exit reaction channels, Ψ_B, Ψ_b, Ψ_A , and Ψ_a are the internal wave functions of the corresponding nuclei, $\Psi_{l_a}(\mathbf{r}_a)$ and $\Psi_{l_b}(\mathbf{r}_b)$ are the wave functions of relative motion; $\theta_{l_a l_a I_1}^{C(\lambda) \rightarrow A+a}$ and $\theta_{l_b l_b I_2}^{C(\lambda) \rightarrow B+b}$ are the reduced width amplitudes of the decay of the CN quasistationary state λ via the channels $C \rightarrow A+a$ and $C \rightarrow B+b$.

Here we define the following angular-momentum coupling scheme:

$$\begin{aligned} \mathbf{I}_1 &= \mathbf{I}_a + \mathbf{I}_A, \quad \mathbf{I}_2 = \mathbf{I}_b + \mathbf{I}_f, \\ \mathbf{I}_C &= \mathbf{I}_1 + \mathbf{I}_a = \mathbf{I}_2 + \mathbf{I}_b, \end{aligned} \quad (34)$$

where l_a and l_b are the orbital angular momenta of the particle relative motion in the entrance and exit channels, and I_1 and I_2 are the total spins of the entrance and exit channels.

Using the partial-wave expansion for the distorted waves, we obtain the transition amplitude for the case when the only one CN resonance is being formed,

$$\begin{aligned} T_{if} &= \sum_{I_1 M_{I_1} I_2 M_{I_2}} \langle I_a M_{I_a} I_A M_{I_A} | I_1 M_{I_1} \rangle \langle I_b M_{I_b} I_f M_{I_f} | I_2 M_{I_2} \rangle \\ &\times \sum_{l_a m_a l_b m_b I_C M_C} \langle I_1 M_{I_1} l_a m_a | I_C M_{I_C} \rangle \langle I_2 M_{I_2} l_b m_b | I_C M_{I_C} \rangle \\ &\times \gamma_{l_a l_a I_1}^{C(\lambda) \rightarrow A+a} (\gamma_{l_b l_b I_2}^{C(\lambda) \rightarrow B+b})^* \left[(E_\lambda - E)^2 + \left(\frac{i}{2} \Gamma_\lambda \right)^2 \right]^{-1} \\ &\times Y_{l_a m_a}^*(\vartheta_{k_a}, \varphi_{k_a}) Y_{l_b m_b}(\vartheta_{k_b}, \varphi_{k_b}), \end{aligned} \quad (35)$$

where the partial width amplitudes $\gamma_{l_a l_a I_1}^{C(\lambda) \rightarrow A+a}$ and $\gamma_{l_b l_b I_2}^{C(\lambda) \rightarrow B+b}$ (corresponding to the decay of the CN quasistationary state λ) are given by

$$\begin{aligned} \gamma_{l_a l_a I_1}^{C(\lambda) \rightarrow A+a} &= \theta_{l_a l_a I_1}^{C(\lambda) \rightarrow A+a} \int i^{l_a} \chi_{l_a}(k_a r_a) \Psi_{l_a}(r_a) \\ &\times Y_{l_a m_a}(\vartheta_{r_a}, \varphi_{r_a}) r_a dr_a. \end{aligned} \quad (36)$$

Now, using the expressions (5), (6), and (35), we can proceed to evaluate the spin tensors $\rho_{kq}(I_f)$ of the density matrix for the case of the only one CN resonance.

In the region of the quasicontinuous spectrum, where different resonances overlap strongly, it is necessary to average the contribution of each resonance over the energy and to sum all resonances in the averaging interval. As a result, instead of the partial widths, we obtain the transmission coefficients $\mathcal{T}_{l_a I_1}^{I_C}$, which are related to the average partial width $|\overline{\gamma_{l_a I_1}^{I_C}}|^2$ and the average spacing D_{I_C} between levels:

$$\mathcal{T}_{l_a I_1}^{I_C} = 2\pi \frac{|\overline{\gamma_{l_a I_1}^{I_C}}|^2}{D_{I_C}}. \quad (37)$$

Finally, spin tensors of the density matrix in the statistical limit of the CN model take the form

$$\begin{aligned} \rho_{kq}(I_f) &= \frac{(2I_f + 1)^{1/2}}{2K_a^2 (2I_A + 1)(2I_a + 1)} \sum_{I_1 I_2 I_2'} (-1)^{2I_C + I_f + I_b} \\ &\times (2I_C + 1)^2 w(I_f I_2 I_2' : I_b k) \\ &\times [(2I_1 + 1)(2I_2 + 1)]^{1/2} (-1)^{m_i + I_1 + I_2 + I_2'} \\ &\times \sum_{l_a l_b l_a' l_b' l_l' m_l m_l'} \frac{\mathcal{T}_{l_a I_1}^{I_C} \mathcal{T}_{l_b I_2}^{I_C}}{G(I_C)} P_{l_b m_l}(\theta_b) P_{l_b' m_l'}(\theta_b) \\ &\times [(2l + 1)(2l' + 1)(2l_a + 1)(2l_b + 1)]^{1/2} \\ &\times \langle l m_l l' - m_l' | k q \rangle \langle l_a 0 l_b - m_l | l m_l \rangle \\ &\times \langle l_a' 0 l_b' - m_l' | l' m_l' \rangle \\ &\times w(I_2 I_2' l' : I_1 k) w(I_1 l_a I_2 l_b : I_C l) w(I_1 l_a' I_2' l_b' : I_C l'). \end{aligned} \quad (38)$$

The denominator $G(I_C)$ in Eq. (38) is referred to as the total decay width of CN and includes all the energetically allowed decay channels of the CN:

$$\begin{aligned} G(I_C) &= \sum_{n l_b} \sum_{I_2 = |l_b - I_C|}^{l_b + I_C} \sum_{I_f = |I_2 - I_b|}^{I_2 + I_b} \\ &\times \left[\sum_{E_f'} \mathcal{T}_{l_b I_2}^{I_C} + \int_{E_c}^{E_f^*} \mathcal{T}_{l_b I_2}^{I_C} \rho(E_f^*, I_f') dE_f^* \right], \end{aligned} \quad (39)$$

where n is the number of open channels, E_f^* is the energy of the excited level of the final nucleus B , and E_c is the energy of the lower edge of the continuum. The transmission coefficients $\mathcal{T}_{l I}^{I_C}$ can be determined through the elastic scattering

matrices of the entrance and exit channels, and can be calculated, for example, by using the optical model of elastic scattering.

Finally, we are able to calculate ACFs by using both the spin tensors of the density matrix (38) and the appropriate expressions (11), (12) for the tensors $\varepsilon_{kq}(I_f)$ of the efficiency matrix.

III. APPLICATION OF THE MODELS AND RESULTS

A. The reaction $^{12}\text{C}(^{14}\text{N},d)^{24}\text{Mg}^*(\alpha)^{20}\text{Ne}$

The first results of studies of nuclear reactions induced by nitrogen ions at incident energies up to 100 MeV on $1p$ -, $2s$ -, and $1d$ -shell nuclei were performed in Refs. [43,44]. It was shown that these reactions could be treated as ones involving the transfer of large group of nucleons. Nevertheless, after further and detailed analysis both of the spectra, the excitation functions, the angular distributions, and the correlations of resonancelike structure in the excitation functions obtained from elastic scattering and from reactions, it was concluded that the mechanism of CN formation plays the dominant role in these reactions [45–48].

However, after analysis of the differential cross sections for these reactions, in Ref. [47] and later in Ref. [28], it was noticed that the angular distributions have a clear oscillated structure. For example, in the $^{12}\text{C}(^{14}\text{N},d)^{24}\text{Mg}^*$ reaction only two differential cross sections for the 5.23-MeV (3^+) and (7.75+7.81)-MeV (1^+ , 5^+) states in ^{24}Mg [47] have a smooth shape symmetrical about 90° . The population of these states is actually not associated with the direct transfer of group of nucleons, owing to the constraints imposed by the spin and parity selection rules. This indicates that the statistical CN model describes only the smooth background, on which oscillations or irregularities associated with other reaction mechanisms are super imposed, the contribution of which can be comparable to that of CN formation. Nevertheless, the substantial contribution of CN mechanism in the reactions induced by nitrogen ions in a wide range of incident energies is reasonable and completely obvious in view of the large number of open decay channels and the high level state density of the CN.

The deuteron angular distribution measurements in the $^{12}\text{C}(^{14}\text{N},d)^{24}\text{Mg}$ reaction and calculations included DWBA and CN analysis [28]. The direct-carbon-transfer calculations have reached the differential cross section with structure, but did not permit to make definite conclusions without an estimation of the spectroscopic factors. We extended the analysis of this reaction using EFR-DWBA [29] and statistical CN model [30] to obtain quantitative spectroscopic information. For this purpose, we calculated the RWAs for the $^{14}\text{N} \rightarrow ^{12}\text{C}_{\text{g.s.}} + d$ ($\Lambda_2=0,2$) vertex and estimated the values of the RWAs $\theta_{I_f \Lambda_1}^{24\text{Mg} \rightarrow ^{12}\text{C} + ^{12}\text{C}}$ for $I_f=0$ ($\Lambda_1=0$) and $I_f=6$ ($\Lambda_1=6$) by comparing the experimental [28] and calculated cross sections. Calculations involving the direct transfer of $^{12}\text{C}_{\text{g.s.}}$ allowed us only to obtain a good agreement with the data for both magnitude and angular distributions assuming the considerable large values of the reduced widths for $^{12}\text{C} \otimes ^{12}\text{C}$ configurations in ^{24}Mg and an important role of

the massive transfer mechanism in the $^{12}\text{C}(^{14}\text{N},d)^{24}\text{Mg}$ reaction.

Measurements of the d - α ACFs in the $^{12}\text{C}(^{14}\text{N},d)^{24}\text{Mg}(\alpha)^{20}\text{Ne}$ reaction for the 13.45-MeV (6^+) state in ^{24}Mg and the theoretical treatment of the ACFs [19] gave reasonable description of the observed oscillated structure of ACFs for this state in ^{24}Mg and provided convincing evidence for the importance of direct ^{12}C cluster transfer in this reaction. The angular distributions in this reaction involving the ground state (g.s.) (0^+) and the first excited (2^+) state in ^{24}Mg have been analyzed by Sakuta *et al.* [49]. A comparison was made between the experimental data and two models, the direct carbon transfer and the direct ^{10}B transfer (the heavy stripping due to break up of the target nucleus ^{12}C). It was demonstrated that the calculations that included these two mechanisms faithfully reproduced the deuteron angular distributions. Whereas the quantitative analysis showed a drastic discrepancy between the spectroscopic amplitudes for the [$^{12}\text{C} \otimes ^{12}\text{C}$] $_{\text{g.s.},2^+}$ configurations calculated in the cluster model and the ones extracted by comparing the calculated and experimental cross sections (by a factor of 10^2). This example gave rise a question of whether the conventional cluster spectroscopic amplitude calculation technique is applicable to describe multinucleon quasimolecular spectroscopic amplitudes?

Our present work contains both a consistent analysis of the deuteron angular distributions and the d - α ACFs in the $^{12}\text{C}(^{14}\text{N},d)^{24}\text{Mg}^*(\alpha)^{20}\text{Ne}_{\text{g.s.}}$ reaction involving a number of the $^{24}\text{Mg}^*$ states beginning from the g.s. and up to the 14.15 MeV, 8^+ state at a few ^{14}N beam energies.

B. Calculation of the reduced width amplitudes

Let us begin from the RWA calculation for the $^{14}\text{N} \rightarrow ^{12}\text{C} + d$ vertex. We use the shell model wave functions of nuclei with the intermediate coupling coefficients $a_{[f_a]L_a S_a T_a}^{J_a T_a}$

$$\begin{aligned} &^{14}\text{N}\{[f_a]L_a S_a T_a; I_a = 1\}: -0.195[442]^{13}\text{S} \\ &\quad + 0.949[442]^{13}\text{D} - 0.247[433]^{11}\text{P}, \\ &^{12}\text{C}\{[f_X]L_X S_X T_X; I_X = 0\}: 0.840[44]^{11}\text{S} - 0.200[422]^{15}\text{D} \\ &\quad + 0.492[431]^{13}\text{P}, \\ &^{12}\text{C}\{[f_X]L_X S_X T_X; I_X = 2\}: 0.899[44]^{11}\text{D} - 0.217[431]^{13}\text{P} \\ &\quad + 0.299[431]^{13}\text{D} + 0.208[431]^{13}\text{F}, \end{aligned}$$

obtained in Ref. [50] by the diagonalization of the Hamiltonian with nucleon-nucleon interaction.

The FPCs for $^{14}\text{N} \rightarrow ^{12}\text{C} + d$ vertex involving the transfer of massive cluster ^{12}C in two intermediate states [g.s. (0^+) and 4.33 MeV (2^+)] are used here to calculate the RWAs $\Theta_{\Lambda_2 I_X I_2}^{14\text{N} \rightarrow ^{12}\text{C} + d}$ [see Eqs. (22), (26)]. The RWA $\Theta_{\Lambda_2 I_X I_2}^{14\text{N} \rightarrow ^{12}\text{C} + d}$ values are presented in Table I.

The RWAs $\Theta_{\Lambda_1 I_1 I_X}^{24\text{Mg} \rightarrow ^{12}\text{C} + ^{12}\text{C}}$ (27) are assumed to be adjusted parameters, which are used for the structure factor $\Theta_{I \Lambda_1 \Lambda_2 I_1 I_2 I_X}$ (16) calculation. Notice that if one takes into

TABLE I. Reduced width amplitudes $\Theta_{\Lambda_2 I_X I_2}^{14N \rightarrow 12C+d}$.

(a)				
$I_X=0$, g.s.				
I_2	0	2		
Λ_2	0	2		
$\Theta_{\Lambda_2 I_X I_2}^{14N \rightarrow 12C+d}$	0.326	0.736		
(b)				
$I_X=2$, $E_f^*=4.44$ MeV				
I_2	2	0	1	2
Λ_2	0	2	2	2
$\Theta_{\Lambda_2 I_X I_2}^{14N \rightarrow 12C+d}$	0.885	0.415	-0.533	0.198

account the higher excited states in transferred $^{12}\text{C}^*$ cluster (for example, 14.08 MeV, 4^+), one needs to calculate the wave functions for the quasistationary states with more accuracy, because the binding energy of the $^{12}\text{C} \otimes ^{12}\text{C}^*$ configurations becomes positive even for the ground state in ^{24}Mg .

We should mention that the differential cross section calculation in EFR-DWBA includes noncoherent sums over total momenta I_1, I_2 and transferred angular momentum l , whereas the expression for ACF contains a noncoherent sum over I_2 and its projectile M_2 , but a coherent summing over total momentum I_1 and its projectile M_1 and over transferred

orbital momentum l . In any case the transition amplitude (15) includes the coherent sums over total momentum I_X of the transferred nucleus and over the relation motion angular momenta Λ_1 and Λ_2 .

C. Differential cross sections

We performed calculations of the differential cross sections at ^{14}N bombarding energies of 29 and 35 MeV for the different excited states in ^{24}Mg , under the assumption of the direct massive cluster transfer model and statistical CN model in the framework of the formalism presented in Sec. II.

The computer code based on the modified HF formalism for the CN model has been used in our calculations (the interested reader can find the CNCOR description in our work [18]). The CNCOR code allows to calculate all the components of the spin tensors of the density matrix for any state in the final nucleus B^* , the differential cross sections of the reaction, and particle-particle and particle- γ quantum angular correlation functions. The optical-model elastic scattering calculations are carried out for the nuclei with arbitrary spins including the spin-orbit interaction. The detailed discussion of parameter choice in the CN calculation has been presented in our previous works [22,30]. The optical potential and HF calculation parameters are shown in Table II.

In the HF formalism of the statistical CN model a special attention has been made to the concept of a critical angular momentum I_{cr} [47,48]. The critical angular momentum I_{cr} ,

TABLE II. CN calculation and interaction potential parameters; $\mathbf{V}(r) = Vf_V^{-1}(r) + iWf_W^{-1}(r) + V_C$, $f_n(r) = 1 + \exp[(r-R_n)/a_n]$, $n = V, W$.

	(a)												
	^{22}Na + α	^{25}Mg + p	^{25}Al + n	^{24}Mg + d	^{12}C + ^{14}N	^{20}Ne + ^6Li	^{23}Na + ^3He	^{21}Ne + ^5Li	^{18}F + ^8Be	^{16}O + ^{10}B	^{21}Na + ^5He	^{19}F + ^7Be	
$a^b(\text{MeV}^{-1})$	4.01	4.56	4.56	4.38	2.55		4.197	3.83	3.285		3.83	3.47	
$\Delta^c(\text{MeV})$	0	1.509	2.051	6.258	0		1.345	2.366	0		2.899	1.279	
$Y^d(\text{MeV})$	0.194	0.157	0.157	0.168	0.412		0.180	0.210	0.271		0.210	0.248	
$E_c^e(\text{MeV})$	4.47	5.01	5.07	10.06	8.98		5.77	5.78	4.96	8.89	6.51	4.683	
N^f	20	18	25	40	18	21	19	35	23	24	50	15	
$V(\text{MeV})$	90.15	42.82	47.0	50.0	100.0	65.5	11.84	11.62	11.67	11.07	54.4	35.4	
$R_V(\text{fm})$	4.33	3.68	3.5	4.33	5.6	4.02	5.786	6.033	6.238	6.310	4.76	4.643	
$a_V(\text{fm})$	0.58	0.67	0.72	0.59	0.48	0.41	0.45	0.45	0.45	0.45	0.53	1.05	
$W(\text{MeV})$	10.8	6.88 ^a	11.3 ^a	16.0	27.0	12.0	1.756	1.687	1.704	1.513	9.8	11.5 ^a	
$R_W(\text{fm})$	4.33	4.15	3.71	4.33	5.92	3.87	5.786	6.033	6.238	6.310	4.76	5.684	
$a_W(\text{fm})$	0.58	0.37	0.47	0.59	0.26	1.48	0.45	0.45	0.45	0.45	0.53	0.62	
$R_C(\text{fm})$	3.36	3.50	0.	4.33	6.58	6.79	5.786	6.033	6.238	6.31	3.92	6.79	
(b)													
Channel	$R_V(\text{fm})$	$a_V(\text{fm})$	$R_C(\text{fm})$										
$d + ^{12}\text{C}$	2.97	0.65	2.97										
$^{12}\text{C} + ^{12}\text{C}$	4.235	0.7	4.235										

^aImaginary wells are of the surface type.

^bThe level density parameter, $a = A/5.48$ [51].

^cThe pairing energy [48].

^dThe yrast-line cutoff parameter is defined as $Y = \hbar^2/2\mathcal{F}_{rig}$, where \mathcal{F}_{rig} is the rigid body moment of inertia; $\mathcal{F}_{rig} = \frac{2}{5}r_0^2 A^{5/3}$, $r_0 = 1.25$ fm.

^eThe energy corresponding to the lower edge of the continuum.

^fNumber of discrete levels.

TABLE III. Grazing and maximum orbital angular momenta (in \hbar units) in the entrance [l_a^{gr} (29 MeV) = 10–11; l_a^{gr} (35 MeV) = 12–13] and exit channels and critical angular momentum of CN.

$I_{24\text{Mg}}^\pi, e^*(\text{MeV})$	29 MeV				35 MeV			
	l_a^{\max}	l_b^{gr}	l_b^{\max}	I_{cr}	l_a^{\max}	l_b^{gr}	l_b^{\max}	I_{cr}
0^+ , g.s.	5	7	5	6	7	7–8	7	8
2^+ , 1.37	7	7	5	8	8	7–8	6	9
2^+ , 4.24	7	6	5	8	8	7	6	9
4^+ , 4.12	7	6	3	8	9	6–7	5	10
3^+ , 5.23					11	7	8	12
6^+ , 8.11; 6^+ , 8.44	9	5	3	10	11	5–6	5	12
6^+ , 13.45	9	2	3	10	10	4	4	11
8^+ , 13.21; 8^+ , 14.15	10	1	2	11	12	4	4	13

as it has been introduced in previous works, determines the possibility of a nuclear fusion in the entrance channel. It depends on the dynamics of the entrance channel and it is considered as the maximum CN angular momentum $I_{cr} = I_C^{\max}$ which is being realized in the reaction. For example, the HF cross sections for the given reaction were calculated in Ref. [47] at the beam energies $E_{lab} = 25$ –40 MeV assuming that all angular momenta in the entrance channel, which do not exceed $I_{cr} = l_a^{gr} - (1-2)\hbar + I_a$, contribute to the ^{26}Al formation (the grazing orbital angular momentum l^{gr} is equal to the orbital angular momentum, for which the transmission coefficient is equal to 0.5 and is given approximately by $l_a^{gr} \simeq K_a R_a$, where K_a is momentum and R_a is interaction radius in the entrance channel). Naturally, I_{cr} was chosen the same for all the excited levels in ^{24}Mg . However, it is necessary to note that the cross sections calculated in the Refs. [47,48] reproduce only the average behavior and considerably overestimate the experimental data for the most levels (especially for the low-lying levels at small angles).

In order to determine correctly the relative contribution of CN and direct mechanisms, let us focus more attention on the choice of I_{cr} . Taking into account that the CN total angular momentum I_C in the channel-spin representation is determined by the selection rules (34), we can conclude that I_{cr} depends on the maximum orbital angular momentum both in the entrance channel and in the exit channel due to the principle of the overall balance,

$$I_{cr} \equiv I_C^{\max} = I_a + I_A + l_a^{\max} = I_b + I_f + l_b^{\max}. \quad (40)$$

In the selected rules (40) one should choose $l_a^{\max} \lesssim l_a^{gr}$ and $l_b^{\max} \lesssim l_b^{gr}$, where l_a^{gr} and l_b^{gr} depend on incident energy. Moreover, l_b^{gr} depends on the energy of the excited state. We also emphasize that the last equivalence in Eq. (40) means that I_{cr} depends on the spin of the final nucleus. In Table III, we present the obtained values of the maximum orbital angular momenta, l_a^{\max} and l_b^{\max} , and the critical angular momentum $I_{cr} = I_C^{\max}$ satisfying the selected rules (40) at incident beam energies 29 and 35 MeV. The grazing orbital angular momentum in the entrance channel l_a^{gr} for these energies is approximately $(10-11)\hbar$ and $(12-13)\hbar$, respectively. At first sight, the result that I_{cr} depends on I_f spin of the final

nucleus (namely, I_{cr} becomes smaller for the low-lying states) seems to be paradoxical, but we should mention that this is a consequence of a formal equivalence of the entrance and exit channels and the selected rules (34), (40). As a result, an effective decrease of l_a^{\max} values for the low-lying levels reduces the CN cross sections for these levels.

Reaction cross section calculations for the direct transfer mechanism were carried out in the EFR-DWBA using the OLYMP-5 computer code [18], which we modified to perform summation over spin I_X of the intermediate nucleus and total angular momenta I_1 and I_2 . The optical-potential and interaction-potential parameters are presented in Table II.

Figures 1 and 2 represent the comparison of the results of CN and EFR-DWBA calculations with the experimental differential cross sections for the $^{12}\text{C}(^{14}\text{N}, d)^{24}\text{Mg}^*$ reaction involving different excited states in ^{24}Mg at beam energies 29 and 35 MeV. The theoretical curves represent the incoherent sum of the CN model and direct massive transfer calculations. We took into account a stripping mechanism of direct transfer of the $^{12}\text{C}^*$ cluster in the g.s. and in the first excited 4.44-MeV (2^+) state.

Our analysis shows that a direct transfer of the ^{12}C cluster provides approximately 80–85 % of the cross section value at forward angles for the g.s. (0^+), 70% for the 1.37-MeV (2^+) level, 50–70 % for the 4.12-MeV (4^+) and 8.11-MeV (6^+) level, and 55–60 % for the 13.45-MeV (8^+) level at 35 and 29 MeV. The CN mechanism produces a major contribution to the cross section at large angles. For the 13.45-MeV (6^+) state a direct-transfer mechanism dominates at any angles, because the CN cross section is small due to the relatively small l_a^{\max} and l_b^{\max} values. One can suggest a certain contribution of the exchange mechanisms (for example, the heavy-particle stripping) at large angles, that arise from the decay of the target nucleus. However, the mechanisms connected with the direct transfer of the ^{10}B cluster are realized due to $^{10}\text{B} \otimes ^{14}\text{N}$ configurations in ^{24}Mg . It is not obviously *a priori* that these configurations are quasimolecular and have comparably big RWAs.

We studied the sensitivity of the results obtained to the variation of our model parameters. It is well known that the absolute value of the cross section in the EFR-DWBA depends on parameters of the relative motion wave functions,

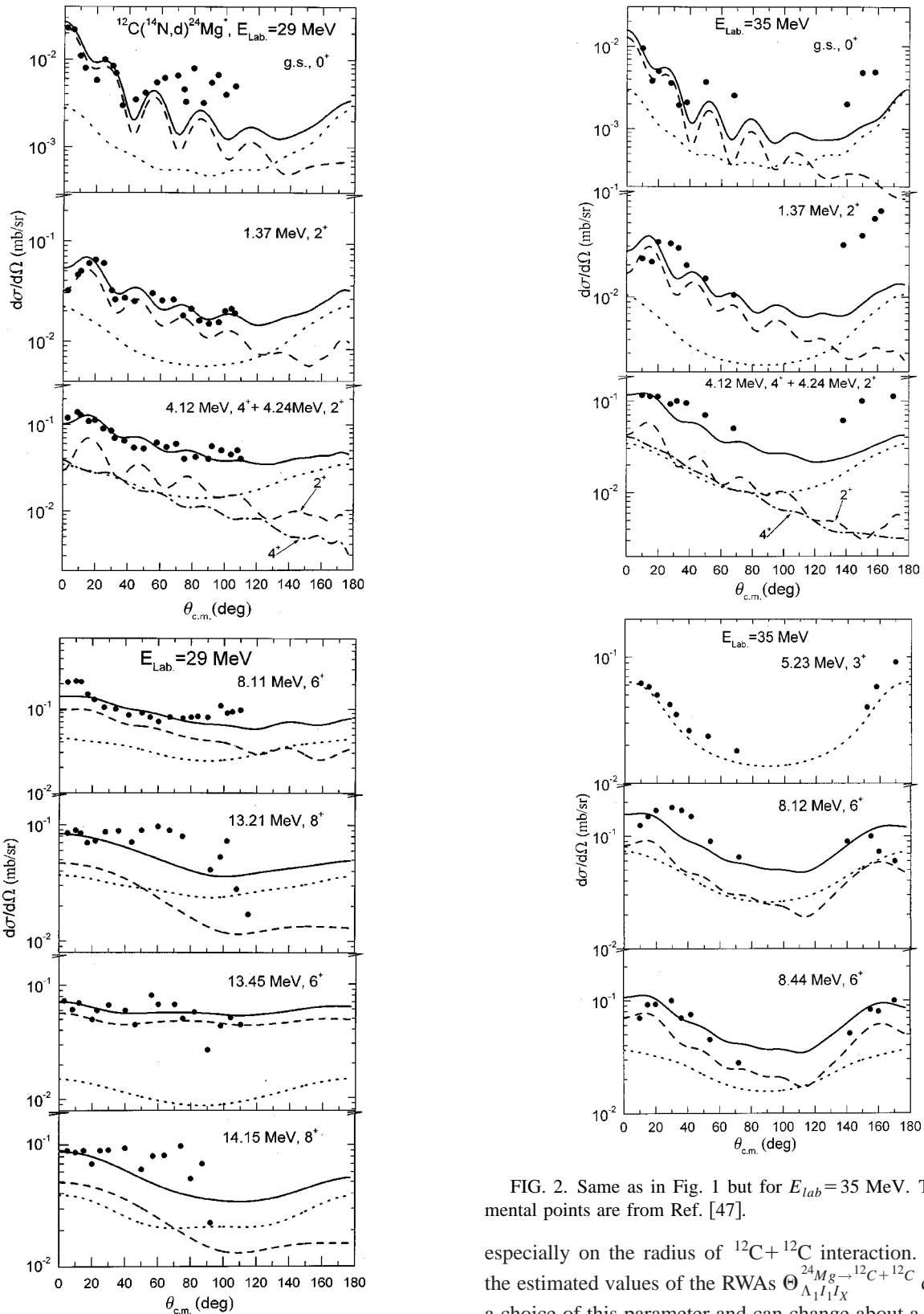


FIG. 1. Deuteron angular distributions for the $^{12}\text{C}(^{14}\text{N},d)^{24}\text{Mg}^*$ reaction at $E_{lab}=29$ MeV calculated for the direct- ^{12}C -transfer mechanism (the dashed curves), CN mechanism (the dotted curves), and for their incoherent sum (the solid curves). The experimental points are from Ref. [28].

FIG. 2. Same as in Fig. 1 but for $E_{lab}=35$ MeV. The experimental points are from Ref. [47].

especially on the radius of $^{12}\text{C}+^{12}\text{C}$ interaction. Naturally, the estimated values of the RWAs $\Theta_{\Lambda_1 I_1 I_X}^{24Mg \rightarrow ^{12}C + ^{12}C}$ depend on a choice of this parameter and can change about a few times with radius variation. In particular, a sufficient increase of the $^{12}\text{C}+^{12}\text{C}$ interaction radius (following Ref. [49]) leads to a decrease of $\Theta_{\Lambda_1 I_1 I_X}^{24Mg \rightarrow ^{12}C + ^{12}C}$ values by factor of 3–5. However, these RWA values are more than the analytical ones (calculated in Ref. [49]) by a factor of 10^2 . The radius of

TABLE IV. Reduced width amplitudes $\Theta_{\Lambda_1 I_1 I_X}^{24Mg \rightarrow 12C+12C}$.

$I_{24Mg}^\pi, \varepsilon^*(\text{MeV})$	I_1	Λ_1	I_X	29 MeV	35 MeV ^a	42 MeV
$0^+, \text{g.s.}$	0	0	0	0.84	0.84	
$2^+, 1.37$	2	2	0	0.66	0.66	
	2	0	2	0	0	
	2	2	2	0.66	0.66	
$2^+, 4.24$	2	4	2	-0.2	-0.2	
	2	2	0	0.66	0.66	
	2	0	2	0	0.2	
$4^+, 4.12$	2	2	2	0.66	0.66	
	2	4	2	-0.2	-0.2	
	4	4	0	0.35	0.35	
$6^+, 8.11; 6^+, 8.44$	4	2	2	0.35	0.35	
	4	4	2	0.35	0.35	
	4	6	2	0	0.35	
$6^+, 13.45$	6	6	0	0	0	0
	6	4	2	0.447	0.447	0
	6	6	2	0.447	0.447	0.447
	6	8	2	0.447	0.447	0.447
	6	6	0	0	0	0
$8^+, 13.21; 8^+, 14.15$	6	4	2	0.114	0.28	0
	6	6	2	0.114	0.28	0.28
	6	8	2	0	0	0.56
	8	8	0	0	0	0
	8	6	2	0.35	0.35	0
	8	8	2	0.35	0.35	0.35
	8	10	2	0	0.35	0.35

^aRWAs for the 13.45-MeV(6^+) state were obtained at $E_{lab} = 33$ MeV and 42 MeV by comparison of calculated and experimental data from Ref. [19].

$^{12}\text{C} + ^{12}\text{C}$ interaction that has been used in our calculations corresponds to the average ^{24}Mg radius and allows one to obtain the all angular distributions and ACFs at given incident energies.

It should also be noted that the angular distributions, their forms, and absolute values depend on the relative contribution of the $^{12}\text{C} \otimes ^{12}\text{C}$ configurations with different $\Theta_{\Lambda_1 I_1 I_X}^{24Mg \rightarrow 12C+12C}$. We have estimated $\Theta_{\Lambda_1 I_1 I_X}^{24Mg \rightarrow 12C+12C}$ values by a comparison of the experimental and calculated differential cross sections and ACFs. The extracted values of RWA $\Theta_{\Lambda_1 I_1 I_X}^{24Mg \rightarrow 12C+12C}$ are shown in Table IV.

Angular distributions for the low-lying levels [g.s., 1.37 and 4.24 MeV (2^+)] have the most pronounced structure. In particular, the best agreement with the experimental data for the states 1.37 MeV and 4.24 MeV (2^+) was obtained under the assumption that the components with $\Lambda_1 = I_f = 2$, $I_X = 0, 2$ introduce the main contribution, whereas the $\Lambda_1 = 0$, $I_X = 2$ component is negligible. A position of the first maximum in angular distributions becomes more correct due to the contribution of the major component with $\Lambda_1 = 4$ ($I_X = 2$).

Angular distributions for the high-lying levels ($E^* \geq 8$ MeV) do not have any distinguish structure, and to ex-

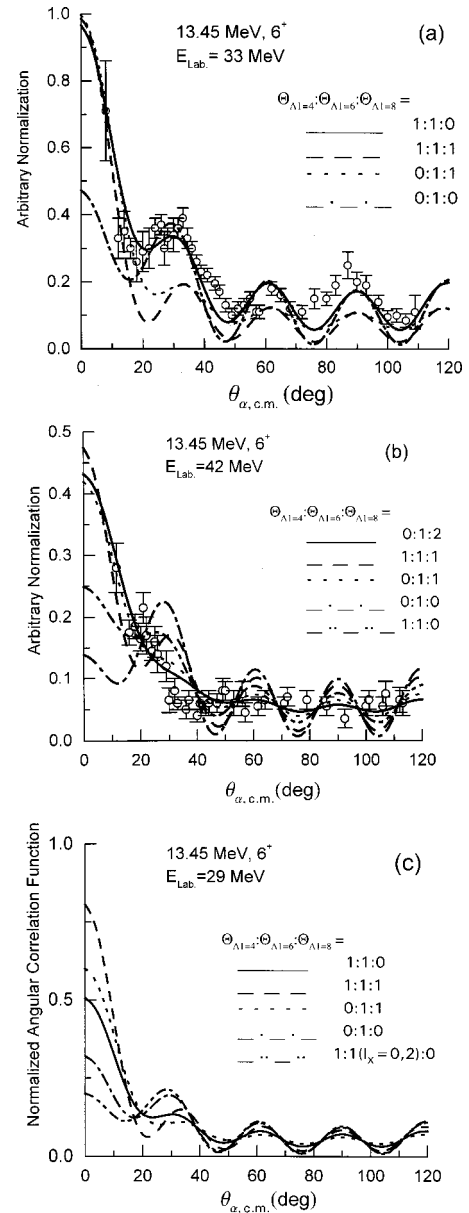


FIG. 3. d - α angular correlation functions for the $^{12}\text{C}(^{14}\text{N},d)^{24}\text{Mg}^*(\alpha)^{20}\text{Ne}$ reaction at beam energies $E_{lab} = 33$ MeV (a), 42 MeV (b), and 29 MeV (c) for the 13.24-MeV (6^+) state in ^{24}Mg at deuteron angle $\theta_{c.m.} = 0^\circ$. The experimental points are from Ref. [19]. Curves represent direct $^{12}\text{C}^*$ ($I_X = 2$) transfer calculations for $^{12}\text{C} \otimes ^{12}\text{C}^*$ configurations corresponding to the different relative weights of $\Theta_{\Lambda_1 I_1 I_X}^{24Mg \rightarrow 12C+12C}$ for $\Lambda_1 = 4, 6, 8$.

tract the RWAs we analyze them simultaneously with the corresponding angular correlation functions.

D. Functions of d - α angular correlation and quasimolecular $^{12}\text{C} \otimes ^{12}\text{C}^*$ states in ^{24}Mg .

The direct- ^{12}C -transfer calculations of ACFs for the excited states in ^{24}Mg [beginning from the 4.12-MeV (4^+) state] have been performed.

In Fig. 3, we compare the calculated ACFs with experimental data [15,19] for the 13.45-MeV (6^+) state in ^{24}Mg at

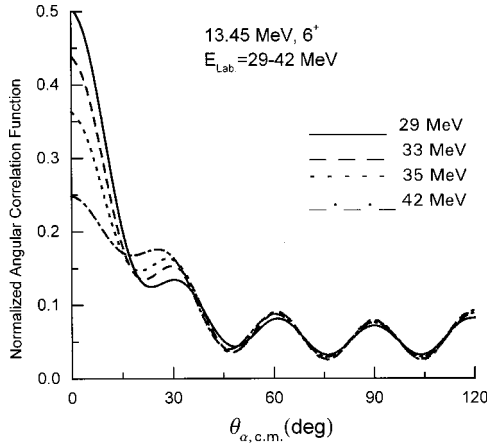


FIG. 4. d - α ACFs for the 13.24-MeV (6^+) state in ^{24}Mg calculated with $\Theta_{\Lambda_1=4}=0.114$; $\Theta_{\Lambda_1=6}=0.114$; $\Theta_{\Lambda_1=8}=0$ at different beam energies.

^{14}N bombarding energies of 33 MeV [Fig. 3(a)] and 42 MeV [Fig. 3(b)], as well as the calculated ACFs at 29 MeV [Fig. 3(c)] for deuteron angle $\theta_{lab}=0^\circ$. Our calculations have been performed for different contributions of the $\Theta_{\Lambda_1 I_1 I_X I_f}^{24\text{Mg} \rightarrow 12\text{C} + 12\text{C}}$ values ($\Lambda_1 = I_f + I_X$).

Two features of the ACFs are worth noting:

(1) The angular dependence of the ACFs with pronounced oscillations is dictated by the values of the projectile energy. Even slight (about 4–5 MeV) changes of the projectile energy can lead to large variations in angular dependence of the ACFs.

(2) The calculated ACFs show a strong sensitivity to the structure of the given excited state in ^{24}Mg , that is, its cluster wave function and a relative weight of the various $^{12}\text{C} \otimes ^{12}\text{C}$ configurations. The latter can be determined by two quantum numbers: the orbital angular momentum Λ_1 of relative motion of two ^{12}C in ^{24}Mg , and the total spin I_X of transferred cluster $^{12}\text{C}^*$ (assuming that $I_A \equiv I_{12\text{C}} = 0$), in accordance with the angular-momentum coupling scheme (29).

At zero-angle deuteron emission the angular-momentum projections $M_f = M_2$ ($M_2 = 0, \pm 1, \pm 2$) are only possible and the ACFs (18) are incoherent sums of squares of spherical harmonics multiplied by the relative populations of the $M_f = M_2$ projections (19). Meanwhile, the M_f projection populations strongly depend on the relative contribution of different [$^{12}\text{C} \otimes ^{12}\text{C}^*$] $_{\Lambda_1 I_1 I_X I_f}$ configurations, which are characterized by the angular-momentum coupling scheme (29). Making a comparison of the calculated ACFs and the experimental ones at different incident energies we were able to restore the cluster structure of a given state and to extract quantitative values of the $\Theta_{\Lambda_1 I_1 I_X}^{24\text{Mg} \rightarrow 12\text{C} + 12\text{C}}$, which are presented in Table IV.

In Fig. 4, the energy dependence of the ACFs for the 13.45-MeV (6^+) state (calculated with the RWAs from Table IV) is shown. Assuming that the orbital rotation of two ^{12}C nuclei relative to each other in a molecular configuration is primarily responsible for the unexpectedly large RWA val-

ues, it should not come as surprise to find that RWAs exhibit a weak energy dependence.

For example, an excellent agreement between the experimental data and theory can be obtained at ^{14}N bombarding energy of 33 MeV, if and only if a coherent summation of two $^{12}\text{C} \otimes ^{12}\text{C}^*$ configurations with $\Lambda_1 = 4, 6$ and $I_X = 2$ is carried out. The $^{12}\text{C}(\text{g.s.})$ transfer with $I_X = 0$ should be limited because the only $\Lambda_1 = I_f = 6$ is allowed in this case. When the beam energy increases up to 42 MeV, the angular dependence of the experimental ACFs becomes smooth and does not show any clear oscillations. To explain this behavior of experimental ACF, we show that the contribution of the higher angular momenta $\Lambda_1 = 6, 8$ becomes more important at high incident energies, which leads to the smoothing of the ACFs. Indeed, if the reaction involves the given excited state, the transferred momentum $\Delta K = K_a - K_b$ rises as the beam energy increases. When multiplied by the interaction radius R , ΔK gives the transferred angular momentum $I = \Lambda_1 + \Lambda_2$. Therefore, we conclude that at the higher incident energy the relevant contribution of the higher allowed transferred angular momenta I and the higher relative motion angular momenta Λ_1 becomes dominant.

For all the levels with one exception [13.45-MeV (6^+) state] the absence of oscillations in ACFs was found by Artemov *et al.* [15]. This fact requires reasonable explanation and justification. Let us consider the results of ACF calculation in the direct-transfer model for the other high-lying excited states in ^{24}Mg between 4- and 14-MeV excitation energy. Results of the direct- ^{12}C -transfer calculations for the 8.11-MeV (6^+) state in ^{24}Mg are shown in Fig. 5(a). There we show the ACFs obtained with different $\Theta_{\Lambda_1 I_1 I_X}^{24\text{Mg} \rightarrow 12\text{C} + 12\text{C}}$ values at ^{14}N bombarding energy of 29 MeV. The ACFs presented in Fig. 5(b) were calculated at energies $E_{lab} = 29, 33, 35$, and 42 MeV assuming the $\Theta_{\Lambda_1 I_1 I_X}^{24\text{Mg} \rightarrow 12\text{C} + 12\text{C}}$ values from Table IV. The ACFs for the 8.11- and 8.44-MeV (6^+) states show a smooth, practically nonoscillated behavior at beam energy 29 MeV if the configurations with $\Lambda_1 = 4, 6, 8$ and $I_X = 2$ have approximately the same weight. At $E_{lab} = 42$ MeV the configurations with the higher angular momenta, $\Lambda_1 = 6, 8$ are dominant.

Figure 6(a) shows the results of ACF calculations for the 13.21-MeV (8^+) state obtained with different $\Theta_{\Lambda_1 I_1 I_X}^{24\text{Mg} \rightarrow 12\text{C} + 12\text{C}}$ values. One can see that the ACFs calculated at $E_{lab} = 29$ MeV with equivalent contribution of the configurations with $\Lambda_1 = 6, 8$ and $I_X = 2$ do not contain any oscillations and are sufficiently smooth. Nevertheless, oscillations can appear at high incident energies, for example, at $E_{lab} = 42$ MeV. As can be seen from Fig. 6(b), the energy dependence of the ACFs for this state calculated with $\Theta_{\Lambda_1 I_1 I_X}^{24\text{Mg} \rightarrow 12\text{C} + 12\text{C}}$ values from Table IV is pronounced.

Finally, we can conclude that the polynomial structure of the ACFs is connected with the orbital rotation of two ^{12}C nuclei relative to each other in a molecular configuration. The experimental ACFs indicate that the distribution of the magnetic populations is not homogeneous and this fact is in contradiction with the statistical CN model. To explain this fact we show that a direct transfer of the massive cluster

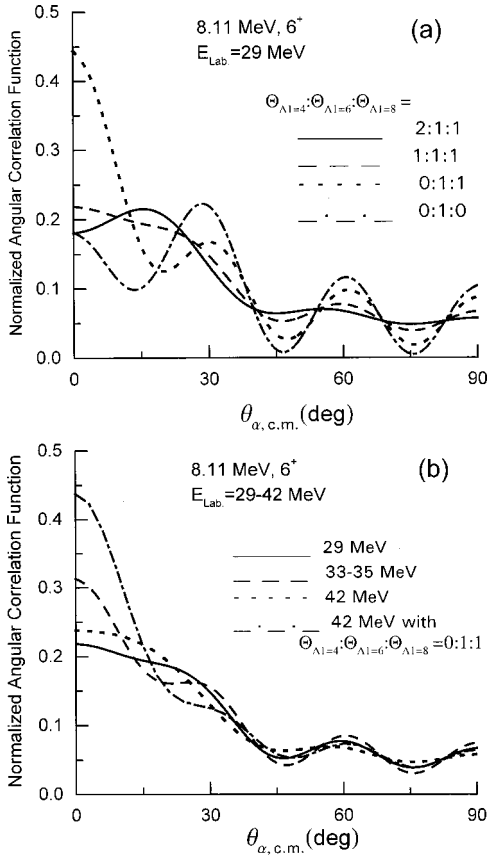


FIG. 5. d - α ACFs for the 8.11-MeV (6^+) state in ^{24}Mg at deuteron angle $\theta_{c.m.} = 0^\circ$. (a) Direct- $^{12}\text{C}^*$ ($I_X = 2$)-transfer calculations at $E_{14N} = 29$ MeV for $^{12}\text{C} \otimes ^{12}\text{C}^*$ configurations corresponding to the different relative weights of $\Theta_{\Lambda_1 I_1 I_X I_f}^{24Mg \rightarrow ^{12}C + ^{12}C}$ for $\Lambda_1 = 4, 6, 8$. (b) Energy dependence of calculated ACFs for $^{12}\text{C} \otimes ^{12}\text{C}$ configuration with $\Theta_{\Lambda_1=4} = \Theta_{\Lambda_1=6} = \Theta_{\Lambda_1=8} = 0.447$.

$^{12}\text{C}^*$ takes place both in the gs and in the first excited 4.44-MeV (2^+) state. For the high-lying levels ($E^* \geq 8$ MeV), with $I_f = 6^+, 8^+$ in ^{24}Mg , the direct transfer of $^{12}\text{C}^*$ in the first excited 4.44-MeV (2^+) state dominates. Populations of the magnetic substates depend on the relative contributions of different $[^{12}\text{C} \otimes ^{12}\text{C}^*]_{\Lambda_1 I_1 I_X I_f}$ configurations with spectroscopic weights determined by the incident energy and transfer momentum. We show that the lower allowed orbital angular momenta of relative motion of two ^{12}C play a dominant role at low energies, whereas at higher energies the higher allowed orbital angular momenta become more important. When the incident energy increases sufficiently, the other intermediate excited states in transferred nucleus are coming into play.

IV. SUMMARY AND CONCLUSION

Based on the theory of the spin density matrix and its spin tensors, we presented the generalized methods for the ACF calculations in the framework of two complementary nuclear reaction models: EFR-DWBA and the modified statistical CN model. The theoretical analysis of the differential cross sections and ACFs in the $^{12}\text{C}(^{14}\text{N}, d)^{24}\text{Mg}(\alpha)^{20}\text{Ne}$ reaction

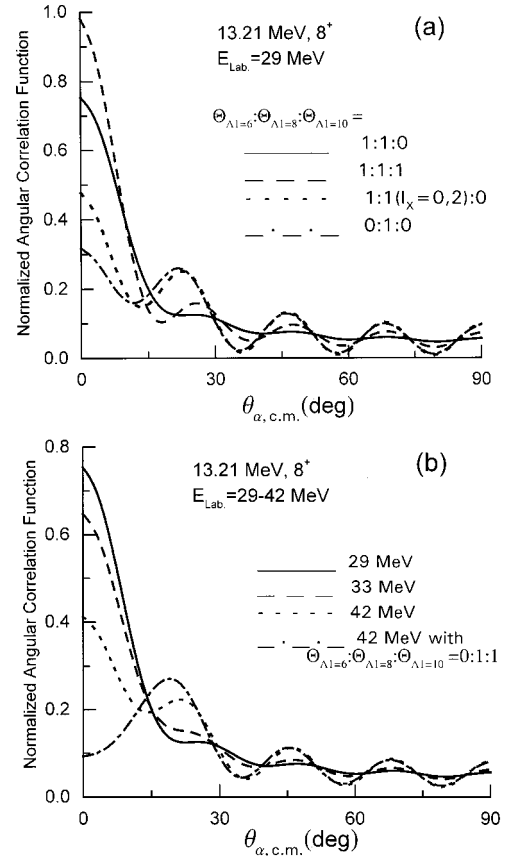


FIG. 6. d - α ACFs for the 13.21-MeV (8^+) state in ^{24}Mg at deuteron angle $\theta_{c.m.} = 0^\circ$. (a) Direct- $^{12}\text{C}^*$ -transfer ($I_X = 2$) calculations at $E_{14N} = 29$ MeV for $^{12}\text{C} \otimes ^{12}\text{C}^*$ configurations corresponding to the different relative weights of $\Theta_{\Lambda_1 I_1 I_X I_f}^{24Mg \rightarrow ^{12}C + ^{12}C}$ for $\Lambda_1 = 6, 8, 10$. (b) Energy dependence of calculated ACFs for $^{12}\text{C} \otimes ^{12}\text{C}$ configuration with $\Theta_{\Lambda_1=6} = \Theta_{\Lambda_1=8} = 0.35$; $\Theta_{\Lambda_1=10} = 0$.

has been performed under the assumption that the direct transfer of $^{12}\text{C}^*$ cluster and CN mechanisms are realized in the reaction, that made it possible to obtain remarkable quantitative agreement between the theoretical calculations and the experimental data. Using the total transferred angular-momentum coupling scheme, we calculated the RWAs for the light vertex $^{14}\text{N} \rightarrow ^{12}\text{C}^* + d$ involving g.s. and 4.44-MeV (2^+) intermediate states in $^{12}\text{C}^*$. It is shown that the contribution of the CN mechanism, which have been calculated taking into account the critical CN angular momentum I_{cr} and the selected rules in the entrance and exit reaction channels, does not exceed 50% of the total cross section value for all the studied excited states in the final $^{24}\text{Mg}^*$ nucleus at beam energies 29 and 35 MeV. Our calculations confirm the existence of the 12-nucleon massive cluster direct-transfer mechanism and substantiate the presence of quasimolecular $^{12}\text{C} \otimes ^{12}\text{C}$ configurations in different states in ^{24}Mg .

The comparison between the existing experimental data and our calculations of the differential cross sections and the ACFs has made possible a direct determination of RWAs for the $^{24}\text{Mg}^* \rightarrow ^{12}\text{C} + ^{12}\text{C}^*$ vertex taking into consideration the different $[^{12}\text{C} \otimes ^{12}\text{C}^*]_{\Lambda_1 I_1 I_X I_f}$ configurations. The calculated $\Theta_{\Lambda_1 I_1 I_X I_f}^{24Mg \rightarrow ^{12}C + ^{12}C}$ values are found to be sufficiently large for

all states we studied and are many times over (by a factor of 10^2) than calculated in the framework of the cluster model [49]. It is shown that large RWA values are associated with relative orbital motion of two ^{12}C with angular momenta Λ_1 in the certain quasimolecular configuration.

We show that the low-lying states in ^{24}Mg [g.s., 1.37 and 4.24 MeV (2^+)] are characterized by the following configurations: $\Lambda_1 = \mathbf{I}_f$, g.s. and 4.44 (2^+) states of intermediate ^{12}C nucleus.

For the 13.45-MeV (6^+) state and the other high-lying states with $I_f = 6^+, 8^+$ in ^{24}Mg all the allowed momenta $\Lambda_1 = \mathbf{I}_f + \mathbf{I}_X$ are involved in the reaction owing to the $^{12}\text{C}(2^+)$ transfer priority. At high incident energies the

higher orbital angular momenta of relative motion Λ_1 are dominant. The energy dependence of ACFs is connected with the spectroscopic amplitude distribution between the different $[^{12}\text{C} \otimes ^{12}\text{C}^*]_{\Lambda_1 I_1 I_X I_f}$ configurations.

ACKNOWLEDGMENTS

The authors are grateful to Dr. E. F. Aguilera and to Professor Yu. F. Smirnov for fruitful discussions and suggestions. T.L.B. acknowledges helpful discussions with Professor V. G. Zelevinsky, Dr. E. Chavez, and Dr. O. Civitarese at the XXV Symposium on Nuclear Physics (Taxco, Mexico, 2002).

-
- [1] D.A. Bromley, J.A. Kuehner, and E. Almqvist, Phys. Rev. Lett. **4**, 365 (1960).
- [2] E. Almqvist, D.A. Bromley, and J.A. Kuehner, Phys. Rev. Lett. **4**, 515 (1960).
- [3] R.R. Betts, S.B. DiCenzo, and J.F. Peterson, Phys. Rev. Lett. **43**, 253 (1979).
- [4] R.W. Zurmuhle, P.H. Kutt, R.R. Betts, S. Saini, F. Haas, and O. Hansen, Phys. Lett. **129B**, 384 (1983).
- [5] S. Saini, R.R. Betts, R.W. Zurmuhle, P.H. Kutt, and B.K. Dichter, Phys. Lett. B **185**, 316 (1987).
- [6] A.H. Wuosmaa, R.W. Zurmuhle, P.H. Kutt, S.F. Pate, and S. Saini, Phys. Rev. Lett. **58**, 1312 (1987).
- [7] N. Curtis *et al.*, Phys. Rev. C **51**, 1554 (1995).
- [8] M. Freer, J.T. Murgatroyd, S.M. Singer, N.G. Curtis, D.J. Henderson, D.J. Hofman, and A.H. Wuosmaa, Phys. Rev. C **63**, 034317 (2001).
- [9] A.H. Wuosmaa, D.J. Hofman, B.B. Back, D.J. Blumenthal, S. Fischer, D.J. Henderson, R.V.F. Janssens, C.J. Lister, V. Nanal, D. Nisius, M.D. Rhein, and P.R. Wilt, Phys. Rev. C **65**, 024609 (2002).
- [10] M. Ohkubo, K. Kato, and H. Tanaka, Prog. Theor. Phys. **68**, 207 (1982).
- [11] K. Kato and H. Tanaka, J. Phys. Soc. Jpn. Suppl. **54**, 136 (1985).
- [12] W. Greiner, J. Y. Park, and W. Scheid, *Nuclear Molecules* (World Scientific, Singapore, 1995).
- [13] R.R. Betts and A.H. Wuosmaa, Rep. Prog. Phys. **60**, 819 (1997).
- [14] N.S. Zelenskaya and I.B. Teplov, Nucl. Phys. **A406**, 306 (1983); Phys. Part. Nucl. **18**, 546 (1987).
- [15] K.R. Artemov, V.Z. Goldberg, M.S. Golovkov, I.P. Petrov, V.P. Rudakov, I.N. Serikov, V.A. Timofeev, H.U. Gersch, and E. Hentschell, Phys. Lett. **149B**, 325 (1984).
- [16] W.D.M. Rae, P.R. Keeling, and S.C. Allcock, Phys. Lett. B **184**, 133 (1987).
- [17] W.D.M. Rae, P.R. Keeling, and A.E. Smith, Phys. Lett. B **198**, 49 (1987).
- [18] T.L. Belyaeva, N.S. Zelenskaya, and N.V. Odintsov, Comput. Phys. Commun. **73**, 161 (1992).
- [19] R.W. Zurmuhle, Z. Liu, D.R. Benton, S. Barrow, N. Wimer, Y. Miao, C. Lee, J.T. Murgatroyd, X. Li, V.Z. Goldberg, and M.S. Golovkov, Phys. Rev. C **49**, 2549 (1994).
- [20] N.S. Zelenskaya and I.B. Teplov, *Characteristics of Excited States of Nuclei and Angular Correlations in Nuclear Reactions* (Energoatomizdat, Moscow, 1995).
- [21] W.R. Falk, R. Aryaeinejad, J.R. Campbell, D.B. Steski, A.A. Mirzai, O.A. Abou-zeid, T.L. Belyaeva, and N.S. Zelenskaya, Nucl. Phys. **A624**, 370 (1997).
- [22] T.L. Belyaeva and N.S. Zelenskaya, Phys. Part. Nucl. **29**, 107 (1998).
- [23] G. Igo, L.E. Hansen, and T.G. Gooding, Phys. Rev. **131**, 337 (1963).
- [24] V.V. Balashov, A.N. Boyarkina, and I. Rotter, Nucl. Phys. **59**, 417 (1964).
- [25] P. Beregi, N.S. Zelenskaya, V.G. Neudatchin, and Yu.F. Smirnov, Nucl. Phys. **66**, 513 (1965).
- [26] A.A. Sakharuk and V. Zelevinsky, Phys. Rev. C **55**, 302 (1997);
- [27] A.A. Sakharuk, V. Zelevinsky, and V.G. Neudatchin, Phys. Rev. C **60**, 014605 (1998).
- [28] K.R. Artemov, M.S. Golovkov, V.Z. Goldberg, V.P. Rudakov, I.N. Serikov, V.A. Timofeev, M. Andrassy, D. Wolfahrt, G.U. Gersch, G. Lang, and E. Hentschell, Yad. Fiz. **44**, 579 (1986) [Sov. J. Nucl. Phys. **44**, 373 (1986)].
- [29] T.L. Belyaeva and N.S. Zelenskaya, Izv. Akad. Nauk SSSR, Scr. Fiz. **52**, 942 (1988) [Bull. Acad. Sci. USSR, Phys. Ser. (Engl. Transl.) **52**, 105 (1988)].
- [30] T.L. Belyaeva, N.S. Zelenskaya, and N.V. Odintsov, Bull. Acad. Sci. USSR, Phys. Ser. (Engl. Transl.) **58**, 112 (1994).
- [31] L.C. Biedenharn and M.E. Rose, Rev. Mod. Phys. **25**, 729 (1953); L. C. Biedenharn, in *Nuclear Spectroscopy*, edited by F. Ajzenberg-Selove (Academic, New York, 1960), Part B, p. 732.
- [32] L.J.B. Goldfarb, in *Nuclear Reactions*, edited by P.M. Endt and M. Demer (North-Holland, Amsterdam, 1959), Vol. 1, p. 159.
- [33] N. Austern, R.M. Drisko, E.C. Halbert, and G.R. Satchler, Phys. Rev. **133**, 3 (1964).
- [34] N.S. Zelenskaya and I.B. Teplov, Fiz. Elem. Chastits At. Yadra **11**, 342 (1980) [Sov. J. Part. Nucl. **11**, 126 (1980)]; *Exchange Processes in Nuclear Reactions* (Moscow State University Press, Moscow, 1985).
- [35] A. de Shalit and I. Talmi, *Nuclear Shell Theory* (Academic, New York, 1963).
- [36] V.G. Neudatchin and Yu.F. Smirnov, *Nucleon Associations in*

- Light Nuclei* (Nauka, Moscow, 1969).
- [37] V.V. Balashov, V.G. Neudachin, Yu.F. Smirnov, and N.P. Yudin, *Sov. Phys. JETP* **37**, 1385 (1959).
- [38] Yu.F. Smirnov and D. Chlebowska, *Nucl. Phys.* **26**, 306 (1961).
- [39] M. Moshinsky, *The Harmonic Oscillator in Modern Physics: From Atoms to Quarks* (Gordon and Breach, New York, 1969).
- [40] Yu.F. Smirnov and M. Moshinsky, *The Harmonic Oscillator in Modern Physics* (Harwood Academic, Amsterdam, The Netherlands, 1996).
- [41] W. Hauser and H. Feshbach, *Phys. Rev.* **87**, 366 (1952).
- [42] N.A. Bogdanova, N.S. Zelenskaya, and I.B. Teplov, *Yad. Fiz.* **50**, 986 (1990) [*Sov. J. Nucl. Phys.* **51**, 631 (1990)].
- [43] N. Marquardt, J.D. Garret, and H.T. Fortune, *Phys. Lett.* **35B**, 37 (1971).
- [44] K. Nagatani, M.J. LeVine, T.A. Belote, and A. Arima, *Phys. Rev. Lett.* **27**, 1071 (1971).
- [45] T.H. Belote, N. Anyas-Weiss, J.A. Becker, J.C. Cornell, P.S. Fisher, P.N. Hudson, A. Menchaca-Rocha, A.D. Panagiotou, and D.K. Scott, *Phys. Rev. Lett.* **30**, 450 (1973).
- [46] D.L. Hanson, R.G. Stokstad, K.E. Erb, C. Olmer, and D.A. Bromley, *Phys. Rev. C* **9**, 929 (1974).
- [47] C. Volant, M. Conjeaud, S. Harar, S.M. Lee, A. Lepine, and E.F. Da Silveira, *Nucl. Phys.* **A238**, 120 (1975).
- [48] H.V. Klapdor, H. Reiss, G. Rosner, and M. Schrader, *Nucl. Phys.* **A244**, 157 (1975); H.V. Klapdor, H. Reiss, and G. Rosner, *ibid.* **A262**, 157 (1976).
- [49] S.B. Sakuta, D.L. Ukrainsky, and Yu.M. Tchuvilsky, *Phys. At. Nucl.* **62**, 1873 (1999).
- [50] A. N. Boyarkina, *Structure of the p-Shell Nuclei* (Moscow State University Press, Moscow, 1973).
- [51] A. Gilbert and A.G. Cameron, *Can. J. Phys.* **43**, 1446 (1965).